2010 American Control Conference
Marriott Waterfront, Baltimore, MD, USA
June 30-July 02, 2010

A Robust-Control-Relevant Model Validation Approach for Continuously Variable Transmission Control

Tom Oomen, Stan van der Meulen, Okko Bosgra, Maarten Steinbuch, and Jos Elfring

Abstract— **High performance continuously variable transmission (CVT) operation requires a reliable control design for its actuation system. The aim of the present paper is to design a high performance robust controller for a range of operating conditions. High performance robust control is achieved by identifying a robust-control-relevant model set that represents the relevant dynamics of the actuation system for a range of operating conditions. Specifically, a new coordinate frame for representing model uncertainty is adopted that transparently connects the size of the model uncertainty and the control criterion, consequently a nonconservative control design can be obtained. Subsequent robust control synthesis reveals that robust performance has been significantly improved over the entire operating range, with respect to both the criterion value and relevant simulated and measured closed-loop step responses.**

I. Introduction

Continuously variable transmissions (CVTs) are power transmission systems that provide infinitely many transmission ratios in a certain range. Advantages of the implementation of such CVTs in passenger cars compared to manual transmissions include improved driving comfort and more efficient use of the internal combustion engine, see also [1].

Performance of the driveline, which includes the internal combustion engine and the CVT, hinges on 1) the accuracy of the achieved transmission ratio, and 2) the efficiency of the CVT. Basically, the CVT is a friction drive and consists of two pairs of conical sheaves with a metal V-belt in between, see Figure 1 and [2]. Variation of the transmission ratio is achieved by translating two of the sheaves. The translation of these sheaves is performed by a hydraulic actuation system. Hence, high performance operation of the CVT requires a high quality controller for the hydraulic actuation system.

The control design involves an inherently multivariable system, since coupling between the sheaves is introduced by the belt that connects them. Additionally, the system dynamics significantly change when the system is operated under different operating conditions, e.g., the coupling introduced by the belt varies for different transmission ratios. Hence, a high quality control design should either adapt to these changes in the system dynamics or be robust against these.

Although many control design approaches, including the approaches in [3] and [4], are available that can deal with this multivariable control problem, these approaches are model-based and thus require a multivariable model of the hydraulic actuation system. In this case, the control performance of the CVT crucially depends on the model that is used during control design. Hence, a high performance model-based control design requires a suitable model.

The dynamical behavior of any physical system, including the CVT, is too complex to be represented exactly by means of a mathematical model. The quality of such inevitably approximate models highly depends on the purpose of the model. In case the goal of the model is subsequent control design, then the model should represent those phenomena that are most relevant for control. This observation has led to the development of control-relevant identification procedures [5], [6], [7], which aim at delivering models that are particularly suitable for subsequent control design. In addition, such system identification methodologies are fast, inexpensive, and generally more accurate in comparison with first principles modeling procedures. For the considered CVT application, such control-relevant identification and control design procedures are capable of delivering controllers that perform well for a specific operating point.

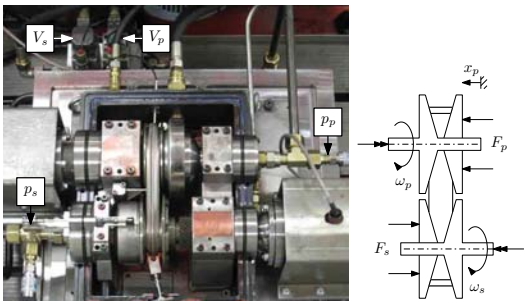

Fig. 1. CVT setup: photograph of experimental setup (left), schematic illustration (right).

Variation of the operating conditions of the CVT leads to a change of the system dynamics, which possibly leads to performance degradation or even closed-loop instability if these variations are not addressed during the control design. The variations of the system dynamics are complex functions of several variables that are hard to determine from measured data. Essentially, this constitutes a nonlinear system identification problem with unknown structure. This motivates the inclusion of these system variations in an uncertainty model, leading to a model set that encompasses the system dynamics over the desired operating range.

Explicit incorporation of an uncertainty model in control-relevant identification procedures has been considered in, e.g., [8]. Although the procedure in [8] can deal with system identification of a model set, the uncertainty is quantified in a coordinate frame that does not transparently connect to the control criterion. As a consequence, the resulting controller generally is unnecessarily conservative.

The main contributions of the present paper include 1) the development of an identification procedure that delivers a robust-control-relevant model set, thereby enabling a non-conservative robust control design; and 2) application of the developed procedure to the design of a robust controller that is guaranteed to deliver high performance for the hydraulic actuation system of a CVT over a range of

The authors are with the Department of Mechanical Engineering, Eindhoven University of Technology, PO Box 513, 5600 MB Eindhoven, The Netherlands, t.a.e.oomen@tue.nl.

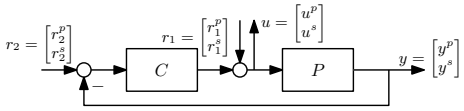

Fig. 2. Controller interconnection structure.

operating conditions. Indeed, high performance control of the multivariable CVT system hinges on the identification of a robust-control-relevant model set. The key to identification of these robust-control-relevant model sets is the development of a coordinate frame for representing model uncertainty that directly connects to the control criterion. As a result, high performance robust controllers that are not unnecessarily conservative can be designed for multivariable systems. Experimental results confirm that the procedure can indeed deliver these robust-control-relevant model sets and enhanced control performance of the CVT hydraulic actuation system.

II. Problem definition

A. Experimental setup

The considered CVT is depicted in Figure 1. The main purpose of the CVT is power transmission, where the torque T and the angular velocity ω for the primary and secondary shaft are indicated with the subscripts p and s, respectively. These variables corresponding to the primary and secondary shaft are related by the transmission ratio. A certain ratio is achieved by applying forces F_p and F_s on the sheaves. These forces are provided by a hydraulic actuation system, where these forces are directly related to pressures p_p and p_s in the primary and secondary hydraulic cylinders, respectively.

The control problem addressed in the present paper is the design of a controller for the hydraulic actuation system, such that it delivers a certain desired pressure. The measured variables y and manipulated variables u are given by

$$y = \begin{bmatrix} p_p & p_s \end{bmatrix}^T, \quad u = \begin{bmatrix} V_p & V_s \end{bmatrix}^T, \tag{1}$$

respectively, where V_p and V_s are the voltages corresponding to the primary and secondary servo valve, respectively. The control of the ratio is achieved by means of a cascade controller, which is discussed in [9].

B. Control goal

The controller interconnection structure is depicted in Figure 2, where P denotes the CVT system and C denotes the feedback controller. The closed-loop transfer function matrix is given by

$$\begin{bmatrix} y \\ u \end{bmatrix} = \begin{bmatrix} P \\ I \end{bmatrix} (I + CP)^{-1} \begin{bmatrix} C & I \end{bmatrix} \begin{bmatrix} r_2 \\ r_1 \end{bmatrix} = T(P, C) \begin{bmatrix} r_2 \\ r_1 \end{bmatrix}. \tag{2}$$

The control criterion and control goal are defined as

$$\mathcal{J}(P, C) = \|WT(P, C)V\|_\infty \tag{3}$$

$$C^{\text{opt}} = \arg\min_C \mathcal{J}(P_o, C), \tag{4}$$

respectively, where W and V are appropriate weighting filters, C^{opt} denotes the optimal controller, and P_o is the true system. Also, $\|.\|_\infty$ denotes the $\mathcal{H}_\infty$-norm, which 1) enables loopshaping-based control designs [10] and 2) is an induced norm enabling the incorporation of model uncertainty. Throughout, all signals and systems evolve in discrete time with a sampling frequency of 1000 [Hz].

C. Robust control

Since the true system P_o is unknown, the optimization problem in (4) cannot be solved directly. To perform the actual optimization, the knowledge of P_o is reflected by a mathematical model. A single model $\hat{P}$ is inevitably an approximation of the true system. This will lead to performance degradation when a controller based on this model, i.e., if

$$C^{\text{NP}} = \arg\min_C \mathcal{J}(\hat{P}, C), \tag{5}$$

is implemented on the true system, then the bound $\mathcal{J}(P_o, C^{\text{NP}}) \geq \mathcal{J}(P_o, C^{\text{opt}})$ holds. To explicitly address the model quality during control design, a model set $\mathcal{P}$ is constructed such that

$$P_o \in \mathcal{P}. \tag{6}$$

This uncertain model set $\mathcal{P}$ is structured as

$$\mathcal{P} = \left\{ P \middle| P = \mathcal{F}_u(\hat{H}, \Delta_u), \|\Delta_u\|_\infty < \gamma \right\}, \tag{7}$$

where Δ_u denotes the model uncertainty, $\hat{H}$ contains $\hat{P}$ and the uncertainty structure, and $\mathcal{F}_u$ denotes the upper linear fractional transformation. Associated with $\mathcal{P}$ is the worst-case performance criterion

$$\mathcal{J}_{\text{WC}}(\mathcal{P}, C) = \sup_{P \in \mathcal{P}} \mathcal{J}(P, C). \tag{8}$$

The worst-case performance criterion (8) in conjunction with the constraint in (6) leads to the performance guarantee

$$\mathcal{J}(P_o, C) \leq \mathcal{J}_{\text{WC}}(\mathcal{P}, C). \tag{9}$$

Hence, the robust control design

$$C^{\text{RP}} = \arg\min_C \mathcal{J}_{\text{WC}}(\mathcal{P}, C) \tag{10}$$

leads to optimal performance for the model set $\mathcal{P}$ and by virtue of (9) to guaranteed performance for P_o.

D. Identification for robust control

Clearly, the performance of the robust controller C^{RP} in (10) crucially depends on the model set $\mathcal{P}$. In case the model set is overly large, then the bound in (9) is not tight and the resulting controller C^{RP} is conservative. To enable high performance robust control, it is desired that $\mathcal{P}$ is robust-control-relevant, i.e., when used for robust control design (10), it leads to a tight bound in (9).

Robust-control-relevant models can be identified by considering the problem dual to (10). Specifically, given a certain C, the robust-control-relevant identification problem is defined by

$$\mathcal{P}^{\text{RCR}} = \arg\min_{\mathcal{P}} \mathcal{J}_{\text{WC}}(\mathcal{P}, C), \tag{11}$$

subject to (6). Note that both C^{opt} and C^{RP} are not available prior to the identification of the model (set), hence these cannot be used in (11). In this case, a possibly moderately performing, stabilizing controller C^{exp} can be used for the identification experiments. Since the choice of this initial controller affects the robust-control-relevant identification criterion in (11), iterating over robust-control-relevant model set identification and robust control design may be required, as is discussed in, e.g., [5], [7], [8].

E. Procedure and outline

A moderately performing, stabilizing controller C^{exp} is already implemented on the experimental setup, leading to the following procedure for the design of a robust controller that achieves guaranteed enhanced performance.

The procedure starts with the identification of a robust-control-relevant model set. In the present paper, first a control-relevant nominal model $\hat{P}$ is identified, see Section III. Second, the nominal model is extended with an uncertainty model in specific robust-control-relevant coordinates, see Section IV. By quantifying the model quality in these robust-control-relevant coordinates, a robust-control-relevant model set is obtained in the sense of (11).

The identified model set is used in a robust control synthesis, see Section V. Performance improvement compared to the initial controller is investigated by means of nominal and robust performance analysis and step responses. Finally, conclusions are drawn in Section VI.

III. Nominal model identification

A. Control-relevant identification

As motivated in Section II-E, first a control-relevant nominal model $\hat{P}$ is estimated. Similar to (11), a control-relevant identification criterion is employed, which is given by

$$\min_{\hat{P}} \|W(T(P_o, C^{\text{exp}}) - T(\hat{P}, C^{\text{exp}}))V\|_\infty, \qquad (12)$$

see [11], [5] for details. In Section IV-A, it is shown that the resulting control-relevant model $\hat{P}$ is useful for constructing robust-control-relevant model sets in the sense of (11).

Observe that (12) involves an $\mathcal{H}_\infty$-norm, which is not straightforward to solve in a system identification procedure. The main idea is to exploit the frequency domain interpretation of the $\mathcal{H}_\infty$-norm to formulate a solvable identification problem. Specifically, under the assumption that C^{exp} internally stabilizes P_o, (12) is equivalent to

$$\min_{\hat{P}} \sup_{\omega\in[0,2\pi)} \bar{\sigma}\left(W(T(P_o, C^{\text{exp}}) - T(\hat{P}, C^{\text{exp}}))V\right) \qquad (13)$$

$$\text{subject to } T(\hat{P}, C^{\text{exp}}) \in \mathcal{RH}_\infty. \qquad (14)$$

Since finite time experiments are performed, $T(P_o, C^{\text{exp}})$ is only identified on a discrete frequency grid. In this case, a lower-bound of the criterion in (12) is used as identification criterion. A sufficiently dense frequency grid should ensure that this lower-bound is tight.

B. Nonparametric identification

In virtue of the control-relevant identification criterion (13), a frequency response function estimate of $T(P_o, C^{\text{exp}})$ is required. Besides the fact that frequency domain identification connects well to the control-relevant identification criterion, frequency domain identification provides the following advantages compared to a time domain approach, see also [12]:

- easy data and noise reduction;
- straightforward combination of multiple data sets, e.g., for multivariable systems.

Note that although $T(P_o, C^{\text{exp}})$ is a closed-loop system, in case the entire closed-loop operator $T(P_o, C^{\text{exp}})$ is identified, then this involves a standard open-loop type of identification problem. In addition, the frequency grid Ω^{id} is used for the identification of a nominal model, containing frequencies in between 0.05 [Hz] and 48 [Hz].

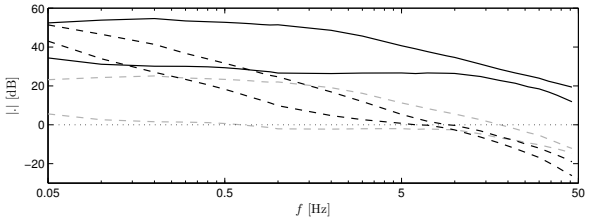

Fig. 3. Identified system $W_{\text{sc}}^{-1}P_o$ (black solid), Scaled system P_o (gray dashed), Shaped system $W_2P_oW_1$ (black dashed).

Regarding the experiment design, two multisine experiments have been performed under normal operating conditions, where each input is excited independently. Each multisine contains the frequencies in Ω^{id} with Schroeder-phases to ensure a low crest factor [12]. The main advantage of multisine inputs is that these reduce the variance of the estimate by averaging of the noise without introducing any bias errors.

C. Weighting filter design

From (13), it is observed that control-relevant identification requires the weighting filters W and V that are later on used in the control design. Clearly, to sensibly define weighting filters, system knowledge is required. In this section, the nonparametric frequency response function estimate, see Section III-B, is employed to design these weights. Specifically, if $T(P_o, C^{\text{exp}})$ is given for $\omega_i \in \Omega^{\text{id}}$, then $P_o(\omega_i),\ \omega_i \in \Omega^{\text{id}}$, is computed using straightforward constant matrix calculations. The resulting nonparametric frequency response function estimate $W_{\text{sc}}^{-1}P_o$ is depicted in Figure 3.

To design the weights, a loopshaping design procedure is adopted as in [10], which is based on shaping the open-loop singular values. Firstly, the system is scaled, specifically, the maximum pressures for p_p and p_s are given by 20 [bar] and 40 [bar], respectively. Hence, the system output is weighted by the constant matrix

$$W_{\text{sc}} = \begin{bmatrix} \frac{1}{20} & 0 \\ 0 & \frac{1}{40} \end{bmatrix}, \qquad (15)$$

see Figure 3 for the singular values of the scaled system. These scaling filters are absorbed into the system, i.e., in the remainder of this paper P_o includes the scaling matrix W_{sc}. Next, as in [10], weighting filters W_2 and W_1 are introduced to specify a desired loop shape. The controller integral action and roll-off are introduced. Additionally, the singular values are aligned at approximately 6 [Hz] to enforce a desired closed-loop bandwidth. In Figure 3, the resulting open-loop shape incorporating the weighting filters W_2 and W_1 is depicted. Given the weighting filters W_2 and W_1, then straightforward algebraic manipulations deliver W and V.

D. Control-relevant coprime factor identification

Given $T(P_o, C^{\text{exp}})$ and weighting filters W and V in Section III-B and Section III-C, respectively, a parametric control-relevant nominal model is estimated. To anticipate on the uncertainty model in Section IV, it is useful to appropriately specify the internal structure of the nominal

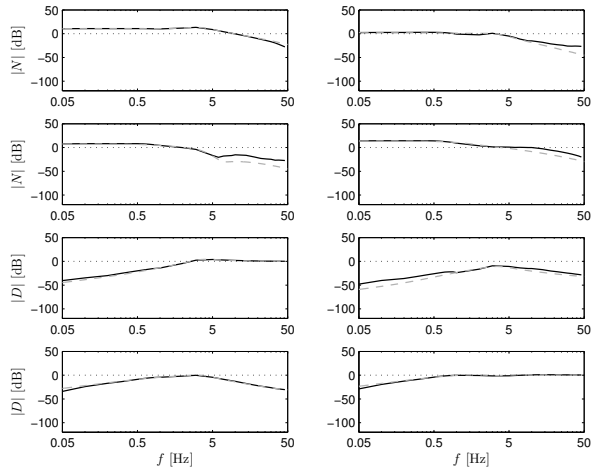

Fig. 4. Identified N_o, D_o (black solid), estimated $\hat{N}, \hat{D}$ (gray dashed).

model $\hat{P}$. Specifically, in [13], [11], it is shown that (13) is equivalent to

$$\min_{\theta} \max_{\omega_i \in \Omega^{\mathrm{id}}} \bar{\sigma} \left(W \left(\begin{bmatrix} N_o(\omega_i) \\ D_o(\omega_i) \end{bmatrix} - \begin{bmatrix} \hat{N}(\theta, \omega_i) \\ \hat{D}(\theta, \omega_i) \end{bmatrix} \right) \right) \quad \text{subject to } \hat{N}, \hat{D} \in \mathcal{RH}_\infty, \tag{16}$$

where the pairs $\{N_o, D_o\}$ and $\{\hat{N}, \hat{D}\}$ are right coprime factorizations of the true system P_o and the model $\hat{P}$, respectively, see, e.g., [4] for a definition. Given C^{exp} and V, $N_o(\omega_i)$ and $D_o(\omega_i)$ can be computed from $T(P_o, C^{\mathrm{exp}})$ for $\omega_i \in \Omega^{\mathrm{id}}$. In Section IV, it is shown that the specific coprime factors in (16) are essential for constructing robust-control-relevant model sets in virtue of (11).

As in [13], a tailor-made parameterization is used to parameterize $\hat{N}$ and $\hat{D}$. As a result, the state dimension of a minimal realization of the coprime factors $\hat{N}$ and $\hat{D}$ is 11, where 5 states originate from the initial controller C^{exp}, 4 states result from the weighting filters, and 2 states result from the parameterization of $\hat{P}$, see also (12). Clearly, the control-relevant coprime factorization of the model has a higher McMillan degree than the nominal model, which is in contrast to, e.g., normalized coprime factors that are used in certain robust control design methodologies [10]. In Section IV-A, it is shown that these additional dynamics are required for constructing a coordinate frame for the uncertainty model that is robust-control-relevant.

A Bode diagram of the identified coprime factor frequency response functions $N_o(\omega_i)$, $D_o(\omega_i)$ and the parametric estimates $\hat{N}$, $\hat{D}$ is shown in Figure 4. The main conclusion is that the parametric model is accurate in the region where the gain of the coprime factors is large, which corresponds to the control-relevant region in view of (16). Note that this corresponds to the desired bandwidth region around 6 [Hz].

IV. Model validation

A. Towards robust-control-relevant model sets

Since the nominal model $\hat{P}$ is not exact, the model quality is taken into account during robust control design by means of an uncertainty model. In addition, the uncertainty model is employed to represent the system variations over the relevant operating range. As already mentioned in Section III-D, coprime factorizations are employed to connect an $\mathcal{H}_\infty$-norm bounded perturbation model to the nominal model $\hat{P}$, see also (7). Specifically, all $P \in \mathcal{P}$ are given by

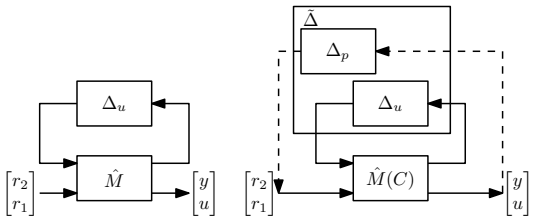

Fig. 5. Left: $\hat{M}$-Δ_u interconnection structure. Right: extended $\hat{M}$-Δ_u interconnection structure.

$$P = (\hat{N} + D_c \Delta_u)(\hat{D} - N_c \Delta_u)^{-1}, \ \Delta_u \in \mathcal{RH}_\infty, \tag{17}$$

where $\{N_c, D_c\}$ is any right coprime factorization of C^{exp}.

The main advantage of the parameterization (17), which is also known as the dual-Youla-Kučera parameterization, is that it only contains models that are stabilized by C^{exp}. In this case, $\mathcal{J}_{\mathrm{WC}}(\mathcal{P}, C^{\mathrm{exp}})$ is always finite for an $\mathcal{H}_\infty$-norm bounded uncertainty model. To illustrate this, observe that for any uncertainty structure, including additive and multiplicative uncertainty [3], the performance under closed-loop with C^{exp} is given by

$$\mathcal{J}(P, C^{\mathrm{exp}}) = \|\hat{M}_{22} + \hat{M}_{21} \Delta_u (I - \hat{M}_{11} \Delta_u)^{-1} \hat{M}_{12}\|_\infty, \tag{18}$$

see Figure 5 (left), where $\hat{M}$ is partitioned according to the signal dimensions as

$$\hat{M} = \left[\begin{array}{c|c} \hat{M}_{11} & \hat{M}_{12} \\ \hline \hat{M}_{21} & \hat{M}_{22} \end{array} \right]. \tag{19}$$

From (18), it is concluded that the performance can become unbounded for some Δ_u in a bounded set $\mathbf{\Delta}_u$. For the model uncertainty structure (17) for any right coprime factorization of $\hat{P}$ and C^{exp}, the performance is given by

$$\mathcal{J}(P, C^{\mathrm{exp}}) = \|\hat{M}_{22} + \hat{M}_{21} \Delta_u \hat{M}_{12}\|_\infty, \tag{20}$$

in which case a norm-bounded Δ_u always leads to a bounded criterion value. The specific coprime factorization $\{\hat{N}, \hat{D}\}$ of $\hat{P}$ that was identified in Section III-D, in conjunction with a specific (W_u, W_y)-normalized coprime factorization of C^{exp}, see [11, Proposition 10] for a state-space computational procedure, leads to the following bound on the worst-case performance

$$\mathcal{J}_{\mathrm{WC}} \leq \|\hat{M}_{22}\|_\infty + \sup_{\Delta_u \in \mathbf{\Delta}_u} \|\Delta_u\|_\infty, \tag{21}$$

see [11]. Note that $\|\hat{M}_{22}\|_\infty = \mathcal{J}(\hat{P}, C^{\mathrm{exp}})$ in (21).

The main result of these new robust-control-relevant coprime factor realizations is that the size of the model uncertainty directly affects the control performance, facilitating the construction of a robust-control-relevant model set in view of (11). Specifically, when estimating model quality, this is done in a coordinate frame that is directly interpretable in terms of the control performance. As a consequence, identification of a robust-control-relevant model set in virtue of (11) is straightforward when compared to other coprime factor realizations and model uncertainty structures.

B. Validation-based uncertainty modeling

In Section III, a nominal model is identified in a certain coprime factor-based coordinate frame. This specific choice leads to the bound (21). As a result, the minimization in (11) is split up in the identification of a nominal model and the quantification of model uncertainty. Up to this point, only the structure of model uncertainty has been determined. Hence, it remains to select the actual size of model uncertainty. Hereto, the validation-based approach in [14] is adopted. The approach is referred to as model validation, since new, independent measurement data are used. By minimizing over the model uncertainty bound γ, i.e.,

$$\gamma(\omega_i) = \bar{\sigma}\left(\Delta_u(\omega_i)\right), \ \forall \Delta_u \in \mathbf{\Delta}_u \tag{22}$$

for all $\omega_i \in \Omega^{\mathrm{id}} \cup \Omega^{\mathrm{val}}$ see also (7), the minimum-norm-validating model uncertainty that can reproduce the measured data is found. Here, Ω^{val} denotes a validation frequency grid containing different frequencies than Ω^{id}. Throughout, it is assumed that Δ_u is unstructured, i.e., $\Delta_u \in \mathcal{RH}_\infty^{n_y \times n_u}$, where $n_x := \dim(x)$ for some vector x.

The result of the validation-based uncertainty modeling approach is both a nonparametric and a parametric bound for the minimum-norm validating Δ_u. Although the nonparametric bound is tighter, the parametric bound is required in subsequent control synthesis.

C. Validation using many data sets

Model validation is performed at other operating conditions, at another frequency grid Ω^{val}, and using different input directions, i.e., the primary and secondary servo valves are actuated simultaneously as, e.g., discussed in [12, Section 2.7]. The result using 31 data sets is depicted in Figure 6.

From Figure 6, it is observed that the use of validation data sets, where a different frequency grid Ω^{val} is adopted in comparison with the frequency grid Ω^{id} in the identification data set, results in significantly larger model uncertainty. The cause can be at least twofold. Firstly, there can be an interpolation error due to the use of a discrete frequency grid in (13). For the considered application, however, the identified frequency response function is relatively smooth and this error is expected to be small. Secondly, by using another input signal, the frequency response function may vary due to the fact that the true system, which is nonlinear, is considered in its linearization around another trajectory. This phenomenon also arises in the identification of the best linear approximation of nonlinear systems, see [12]. It is expected that the latter phenomenon dominates the former phenomenon for this particular application.

To enable control synthesis using the not-invalidated model set, the nonparametric results in Figure 6 are overbounded by a bistable parametric overbound, resulting in the model set $\mathcal{P}^{\mathrm{val}}$. In [11], it is shown using a Nevanlinna-Pick interpolation argument that the resulting model set also is not-invalidated. The main advantage of the robust-control-relevant coordinate frame is that the parametric overbound should be tight in the region where the nonparametric bound γ is largest. This is exactly what is achieved by the second order bistable overbound in Figure 6.

V. Robust control design

Given the robust-control-relevant model set $\mathcal{P}^{\mathrm{val}}$, the next step is to synthesize a robust controller. To perform the actual minimization in (10), note that Figure 5 (left) can be recast into Figure 5 (right). Due to the fact that $\|\Delta_u\|_\infty < 1$ due to the parametric overbound, this involves a skewed-μ problem, see [15]. To perform the actual optimization, a suitable generalization of the $D-K$-iteration, see [4], has been developed. For comparison, also the controller is computed that minimizes the nominal performance cost in (5) using standard $\mathcal{H}_\infty$-optimization algorithms, see [4].

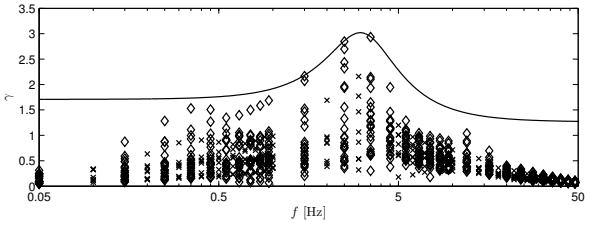

Fig. 6. Resulting γ as a function of frequency from model validation procedure: data sets on identification grid ($\times$), data sets on validation grid ($\diamond$), parametric overbound resulting in $\mathcal{P}^{\mathrm{val}}$ (black solid).

TABLE I
Identification and control synthesis results.

	Minimized criterion	$\mathcal{J}(\hat{P}, C)$	$\mathcal{J}_{\mathrm{WC}}(\mathcal{P}^{\mathrm{val}}, C)$
C^{exp}	-	6.14	7.98
C^{NP}	$\mathcal{J}(\hat{P}, C)$	1.77	∞
$C^{\mathrm{RP,val}}$	$\mathcal{J}_{\mathrm{WC}}(\mathcal{P}^{\mathrm{val}}, C)$	3.57	4.09

The results of the control synthesis are presented in Table I. The following observations are made.

1) Regarding the identification of a robust-control-relevant model set using C^{exp}, it is observed that the nominal model $\hat{P}$ in conjunction with the feedback controller C^{exp} achieves a nominal performance of $\mathcal{J}(\hat{P}, C^{\mathrm{exp}}) = 6.14$. After application of the validation-based uncertainty modeling procedure in Section IV, the worst-case performance of the experimental controller C^{exp} over the model set equals $\mathcal{J}_{\mathrm{WC}}(\mathcal{P}^{\mathrm{val}}, C^{\mathrm{exp}}) = 7.98$. Clearly, using the norm-bound on γ, which equals 3.02, the bound (21) holds.

2) The controller C^{NP}, which obtains optimal performance for the nominal model $\hat{P}$, results in a control criterion of $\mathcal{J}(\hat{P}, C^{\mathrm{NP}}) = 1.77$. Hence, the controller has been significantly improved compared to C^{exp} in terms of the control criterion. However, this performance increase comes at the expense of robustness. Indeed, the worst-case performance $\mathcal{J}_{\mathrm{WC}}(\mathcal{P}^{\mathrm{val}}, C^{\mathrm{exp}}) = 7.98$ has degraded to an unbounded $\mathcal{J}_{\mathrm{WC}}(\mathcal{P}^{\mathrm{val}}, C^{\mathrm{NP}})$, implying that C^{NP} does not stabilize all models in $\mathcal{P}^{\mathrm{val}}$.

3) The controller $C^{\mathrm{RP,val}}$ explicitly addresses all system variations over the desired operating range during control synthesis. Since it is designed to minimize $\mathcal{J}_{\mathrm{WC}}(\mathcal{P}^{\mathrm{val}}, C)$, the bounds $\mathcal{J}_{\mathrm{WC}}(\mathcal{P}^{\mathrm{val}}, C^{\mathrm{RP,val}}) \leq \mathcal{J}_{\mathrm{WC}}(\mathcal{P}^{\mathrm{val}}, C^{\mathrm{exp}})$ and $\mathcal{J}_{\mathrm{WC}}(\mathcal{P}^{\mathrm{val}}, C^{\mathrm{RP,val}}) \leq \mathcal{J}_{\mathrm{WC}}(\mathcal{P}^{\mathrm{val}}, C^{\mathrm{NP}})$ hold.
The main conclusion is that the controller $C^{\mathrm{RP,val}}$ achieves the best performance for the entire range of operating conditions.

A. Controller results

1) Simulation results: First, the synthesized controllers are evaluated using the identified nominal model in Section III. In Figure 7, closed-loop step responses are depicted using $\hat{P}$, i.e., the transfer function $r_2 \mapsto y$ is considered, see also (2). Especially in the top left figure, it is observed that

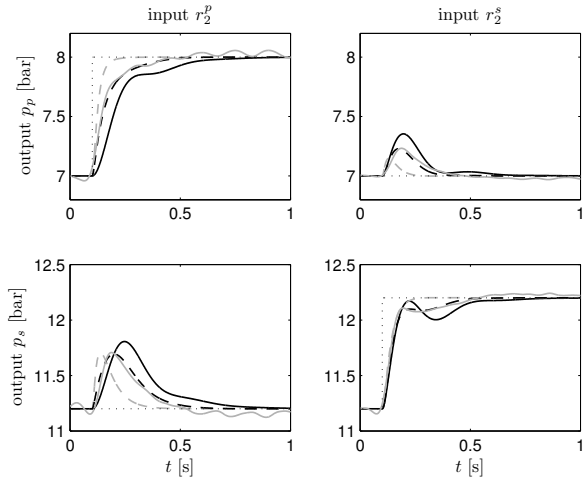

Fig. 7. Closed-loop step responses ($r_2 \mapsto y$): simulation using initial controller C^{exp} (black solid), simulation using optimal nominal controller C^{NP} (gray dashed), simulation using optimal robust controller $C^{\mathrm{RP,val}}$ (black dashed), experimental result using optimal robust controller $C^{\mathrm{RP,val}}$ (gray solid).

decreasing criterion values $\mathcal{J}(\hat{P}, C)$ in Table I correspond to reduced rise times, which is a desired and expected property of the control criterion. In addition, it is observed that all synthesized controllers reduce the oscillations that are especially pronounced in the bottom right figure of Figure 7 when the controller C^{exp} is evaluated. This reduction of oscillations is attributed to the inherently multivariable character of the resulting controllers.

2) Experimental results: Next, the optimal robust controller $C^{\mathrm{RP,val}}$ is implemented on the true system. A comparison with C^{NP} is not performed, since this controller does not satisfy the robust stability condition. The resulting step response is also depicted in Figure 7.

It is observed that the simulation results reliably predict the response obtained with the experimental implementation of $C^{\mathrm{RP,val}}$. Although the responses are not provided in this paper, similar results have been obtained for the initial controller C^{exp}. Hence, the identified model is indeed accurate for control and the robust controller is able to improve the performance under nominal operating conditions. In addition, it is observed that in contrast to the simulations, the experimental results reveal an oscillatory behavior. This behavior is attributed to disturbances caused by centrifugal effects in the hydraulic cylinders, see [9] for an explanation. Although not presented in the present paper, similar results have been obtained under other operating conditions.

VI. Discussion

In this paper, a high performance, robust, and multivariable controller is designed for a CVT hydraulic actuation system through the identification of a robust-control-relevant model set. Specifically, a new robust-control-relevant coordinate frame has been employed to characterize model uncertainty, leading to a transparent connection between the size of the uncertainty and the control criterion. As a result of the parsimonious model set, a nonconservative control design is obtained. Model uncertainty has been included to address both undermodeling as well as changing system dynamics for various operating conditions. As a result, robust performance is significantly increased in comparison with the initial control design. In addition, robustness is significantly increased compared to a nominal control design that does not satisfy the robust stability condition. The optimal (robust) control designs are inherently multivariable, which is a result of the inherent interaction that is present in the CVT.

Implementation of the optimal robust controller on the true system confirms performance improvement. In addition, the closed-loop measured step responses are predicted accurately by the nominal model, which confirms control-relevance.

Regarding the results in the present paper, further performance improvement can be obtained by 1) considering an iterative model set and robust control design procedure, since the present definition of robust-control-relevance depends on the experimental controller; 2) considering two degrees-of-freedom controller implementations of the loopshaping controller; 3) more accurate overbounds of the robust-control-relevant model uncertainty; 4) incorporating structure in the model uncertainty block, which is at the expense of more involved model validation and control synthesis algorithms; and 5) ensuring robustness with respect to product variability by using validation data sets of multiple CVT systems.

Acknowledgements

The authors acknowledge fruitful discussions with Sander Quist, Robbert van Herpen, and Bram de Jager.

References

[1] R. Pfiffner and L. Guzella, "Optimal operation of CVT-based powertrains," *Int. J. Rob. Nonlin. Contr.*, vol. 11, no. 11, pp. 1003–1021, 2001.

[2] G. Lechner and H. Naunheimer, *Automotive Transmissions: Fundamentals, Selection, Design and Application*. Berlin, Germany: Springer, 1999.

[3] S. Skogestad and I. Postlethwaite, *Multivariable Feedback Control: Analysis and Design*, 2nd ed. West Sussex, UK: John Wiley & Sons, 2005.

[4] K. Zhou, J. C. Doyle, and K. Glover, *Robust and Optimal Control*. Upper Saddle River, NJ, USA: Prentice Hall, 1996.

[5] R. J. P. Schrama, "Accurate identification for control: The necessity of an iterative scheme," *IEEE Trans. Automat. Contr.*, vol. 37, no. 7, pp. 991–994, 1992.

[6] M. Gevers, "Towards a joint design of identification and control ?" in *Essays on Control : Perspectives in the Theory and its Applications*, H. L. Trentelman and J. C. Willems, Eds. Boston, MA, USA: Birkhäuser, 1993, ch. 5, pp. 111–151.

[7] P. Albertos and A. Sala, Eds., *Iterative Identification and Control*. London, UK: Springer, 2002.

[8] R. A. de Callafon and P. M. J. Van den Hof, "Suboptimal feedback control by a scheme of iterative identification and control design," *Math. Mod. Syst.*, vol. 3, no. 1, pp. 77–101, 1997.

[9] S. van der Meulen, B. de Jager, E. van der Noll, F. Veldpaus, F. van der Sluis, and M. Steinbuch, "Improving pushbelt continuously variable transmission efficiency via extremum seeking control," in *Proc. 2009 Multi-conf. Syst. Contr.*, Saint Petersburg, Russia, 2009, pp. 357–362.

[10] D. C. McFarlane and K. Glover, *Robust Controller Design Using Normalized Coprime Factor Plant Descriptions*, ser. LNCIS. Berlin, Germany: Springer-Verlag, 1990, vol. 138.

[11] T. Oomen, R. van Herpen, and O. Bosgra, "Robust-control-relevant coprime factor identification with application to model validation of a wafer stage," in *15th IFAC Symp. Sys. Id.*, Saint-Malo, France, 2009, pp. 1044–1049.

[12] R. Pintelon and J. Schoukens, *System Identification: A Frequency Domain Approach*. New York, NY, USA: IEEE Press, 2001.

[13] T. Oomen and O. Bosgra, "Robust-control-relevant coprime factor identification: A numerically reliable frequency domain approach," in *Proc. 2008 Americ. Contr. Conf.*, Seattle, WA, USA, 2008, pp. 625–631.

[14] ——, "Well-posed model uncertainty estimation by design of validation experiments," in *15th IFAC Symp. Sys. Id.*, Saint-Malo, France, 2009, pp. 1199–1204.

[15] M. K. H. Fan and A. L. Tits, "A measure of worst-case $\mathcal{H}_\infty$ performance and of largest unacceptable uncertainty," *Syst. Contr. Lett.*, vol. 18, no. 6, pp. 409–421, 1992.